

COMITATO NAZIONALE PER L'ENERGIA NUCLEARE  
Laboratori Nazionali di Frascati

LNF - 66/4  
4 Febbraio 1966

**G. Barbiellini, C. Bernardini, F. Felicetti and G. P. Murtas:  
PHOTODISINTEGRATION OF THE DEUTERON BY POLARIZED  
 $\gamma$  RAYS. -**

**(Nota interna: n. 305)**

Laboratori Nazionali di Frascati del C.N.E.N.  
Servizio Documentazione

LNF-66/4

Nota interna: n. 305  
4 Febbraio 1966

G. Barbiellini, C. Bernardini, F. Felicetti and G.P. Murtas: PHOTODISINTEGRATION OF THE DEUTERON BY POLARIZED  $\gamma$  RAYS.

## 1 - INTRODUCTION -

Deuteron photodisintegration has been extensively investigated in the past years: a complete reference index can be found in the report by M.E. Toms<sup>(1)</sup>.

### a) - Theory -

The photodisintegration problem looks at first quite similar to the usual photoelectric effect in atoms. There a knowledge of the static (Coulomb) potential between bound charges allows a very accurate computation of the cross section. Corrections arising from the interaction of the incoming  $\gamma$  ray with extra-charges brought in by vacuum polarization do not change in a relevant way the results concerning the photoelectric effect.

In the case of photodisintegration, however, the presence of charged field particles in the two nucleon interaction leaves serious doubts on a description of the process based on the use of a nucleon-nucleon potential. In fact the charge in the deuteron is not strongly localized on the proton but can travel from one nucleon to the other for a substantial fraction of the time in the form of charged exchange meson currents.

It is expected on qualitative grounds that because of the pion mass, the charge can be considered as localized on the average on the nucleons when the frequency  $k$  of the incoming  $\gamma$  ray is such that  $k \ll m_\pi$  ( $\hbar = c = 1$ ). That is when  $k$  is well below the  $\pi$  meson threshold.

Low energy theoretical results ( $< 10$  MeV) are in good agreement with the static potential picture. A very refined calculation of this kind has been recently performed by Partovi<sup>(2)</sup> using the well known multipole series technique. The number of involved multipoles is quite high in order to give results accurate to  $k \lesssim 100$  MeV (in the frame of the static potential picture).

Even a careful analysis like Partovi's one (or the recent work by Le Bellac, Renard, Tran Thanh Van including relativistic corrections<sup>(3)</sup>) is not able to reproduce the high energy data. A peak appears (see fig. 1) in the total cross section at  $k = 250$  MeV and this seems unambiguously related to the first nucleon resonance,  $N^*$ .

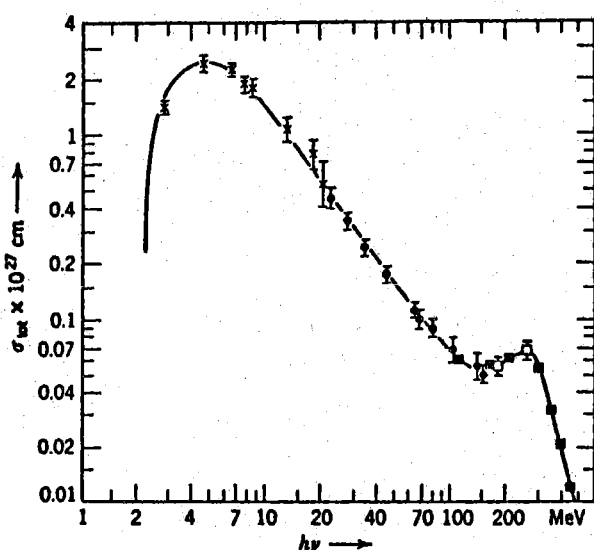


FIG. 1 - Total cross section for deuteron photodisintegration as a function of laboratory photon energy.

After some attempts to interpret the peak on a field theoretical basis (Austern<sup>(4)</sup>, Zachariasen<sup>(5)</sup>) a phenomenological model by Wilson<sup>(6)</sup> succeeded to give a good fit to the total cross section (fig. 2). The phenomenological input to this model is given by the  $\pi$  photoproduction data together with the assumption that every  $\pi$  is reabsorbed by one of the nucleons if they met in a given range.

Giving credit to this model, a dominance of  $N^*$  and S wave production is recognized as compared to the classical photoelectric mechanism (e.m. part).

The interpretation of the angular distribution data appears a bit more complicate: the role of interference terms between e.m. and mesonic contributions is not clear. The same applies to the recent asymmetry data from polarized  $\gamma$  rays (Liu<sup>(7)</sup>, this experiment).

Concerning the asymmetry parameter  $\Sigma(k, \theta)$  defined by

$$(1) \quad \Sigma(k, \theta) = \frac{1}{P} \frac{d\sigma_{||}(P, k, \theta) - d\sigma_{\perp}(P, k, \theta)}{d\sigma_{||}(P, k, \theta) + d\sigma_{\perp}(P, k, \theta)}$$

where

$P$  = polarization of the (linearly polarized)  $\gamma$  rays  
 $\theta$  = c.m. proton angle

$d\sigma_{n(\perp)}$  = differential photodisintegration cross section for production plane parallel (orthogonal) to the polarization vector.

one can definitely say that the results of calculations including only e. m. contributions markedly disagree with the experimental results at energies  $\gtrsim 80$  MeV.

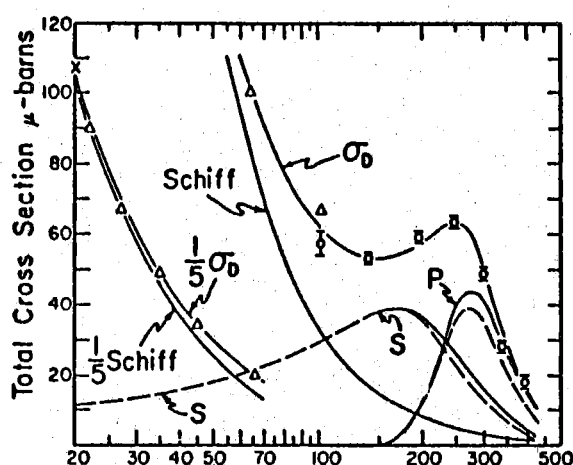


FIG. 2 -  $\sigma_D$  line is according to the Wilson<sup>(6)</sup> model. The curve marked "Schiff" shows the result of a calculation which neglects specific meson effects<sup>(14)</sup>.

behaviour as a function of the c.m. proton angle at the resonance. This can be attributed to magnetic dipole absorption as expected if the  $N^*$  contributes.

We are mainly concerned with measurements of the asymmetry parameter  $\Sigma(k, \theta)$  in the energy range in which meson currents play the relevant role; previous measurements of  $\Sigma$  have been published by Liu<sup>(7)</sup> for the  $\theta$  values  $45^\circ$ ,  $90^\circ$ ,  $135^\circ$  and  $k \lesssim 230$  MeV, that is just below the resonant peak.

## 2 - THE EXPERIMENTAL APPARATUS -

A polarized  $\gamma$  ray beam is one of the facilities of the Frascati electron synchrotron (Barbiellini et al.<sup>(8)</sup>). This beam is obtained by the crystal technique whereas the beam used by Liu is obtained by the angular sampling technique (Mozley et al.<sup>(9)</sup>). In both cases the head of the  $\gamma$  ray spectrum is at higher energies than those of the polarized  $\gamma$  rays so that a selection of the pho-

We will present in § 3 and fig. 10 a curve for the asymmetry function  $\Sigma$  computed in the spirit of the Wilson model: this interpolation seems to indicate that a simple phenomenological description giving a dominant role to mesonic contributions should be possible.

### b) - Experiments -

Results on the photodisintegration cross section have been published by many authors: note in particular in the Toms recollection<sup>(1)</sup> the work by Keck and Tollestrup extending to  $k = 450$  MeV(x).

Besides the already mentioned peak at  $k = 250$  MeV, the cross section shows a peculiar  $2 + 3 \sin^2 \theta$  behaviour as a function of the c.m. proton angle at the resonance. This can be attributed to magnetic dipole absorption as expected if the  $N^*$  contributes.

(x) - Recent data by a group at Bonn (1965 Hamburg Conference) disagree with all previous results. As far as we know this discrepancy is not yet understood.

to disintegration among  $\pi$  photoproduction processes (f.p. $\pi$ ) is desirable when f.p. $\pi$  comes into play. This fact limits the maximum energy at which Liu can work with single particle detection (because of Linac's duty cycle difficulty). Here at Frascati the  $\gamma$  beam pulse length is  $\sim 2$  msec allowing for neutron-proton coincidences so that the energy range can be extended to about 400  $\div$  450 MeV as can be deduced from the beam polarization data (see fig. 3).

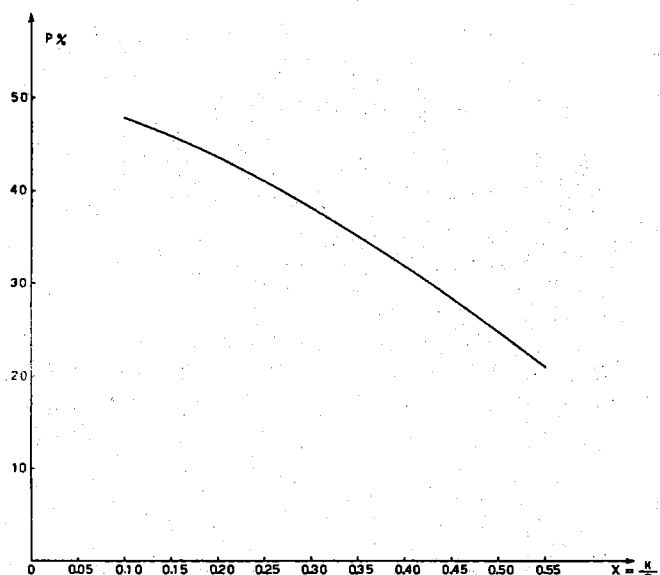


FIG. 3a)

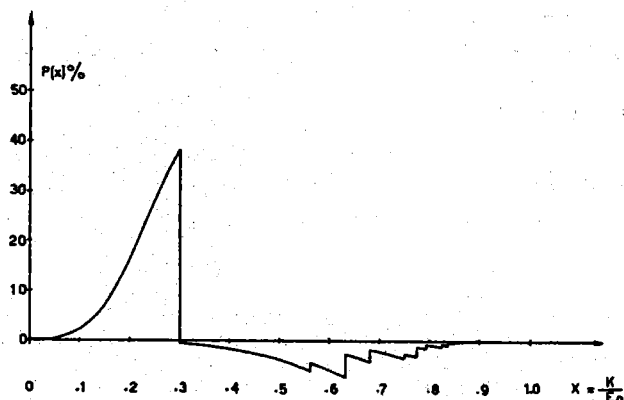


FIG. 3b)

FIG. 3 - a), b), Beam polarization data.

$A S_2$  is a 3 cm thick lead absorber to eliminate soft charged particles;  
 $S_4$  is a  $25 \times 25 \times 1$ ,  $\text{cm}^3$  plastic, 50 cm far from the target (in anticoincidence);  
 $S_5$  is a liquid (NE 213) cylindrical neutron counter, 25 cm deep, 20 cm base diameter.

In fig. 8 the block scheme of electronics is given. The spark chamber is triggered by  $(S_1 + S_2 + \bar{S}_3 + S_5) - (S_1 + S_2 + \bar{S}_3 + S_5 + \bar{S}_4)$ .

The contamination to be expected in the p-n coincidences due to f.p. $\pi$  has been estimated by using the total f.p. $\pi$  cross section (White et al. (10)) and a phase space distribution of the reaction products. This contamination is completely negligible.

Figs. 4, 5, 6 show the relevant kinematics of the photodisintegration and f.p. $\pi$  processes.

Fig. 7 shows the experimental apparatus used in this experiment: it consists of a proton range telescope  $S_1 S_2 (S.C.) S_3$  ( $S$  are scintillation counters, (S.C.) a multi-plate spark chamber) and a neutron counter  $\bar{S}_4 S_5$  on the other side.

Detailed characteristics are as follows:

$S_1$  is a  $16 \times 16 \times 1 \text{ cm}^3$  plastic, 160 cm far from the target;  
 $A S_1$  is a wedge shaped aluminium absorber,  $9,9 \text{ gr/cm}^2$  thick at center;  
 $S_2$  is a  $20 \times 20 \times 1.25 \text{ cm}^3$  plastic;  
S.C. is a  $29 \times 29 \text{ cm}^2$  front area spark chamber, (31 plates, 1 mm Al each);  
 $\bar{S}_3$  is a  $29 \times 29 \times 1 \text{ cm}^3$  plastic (in anticoincidence);

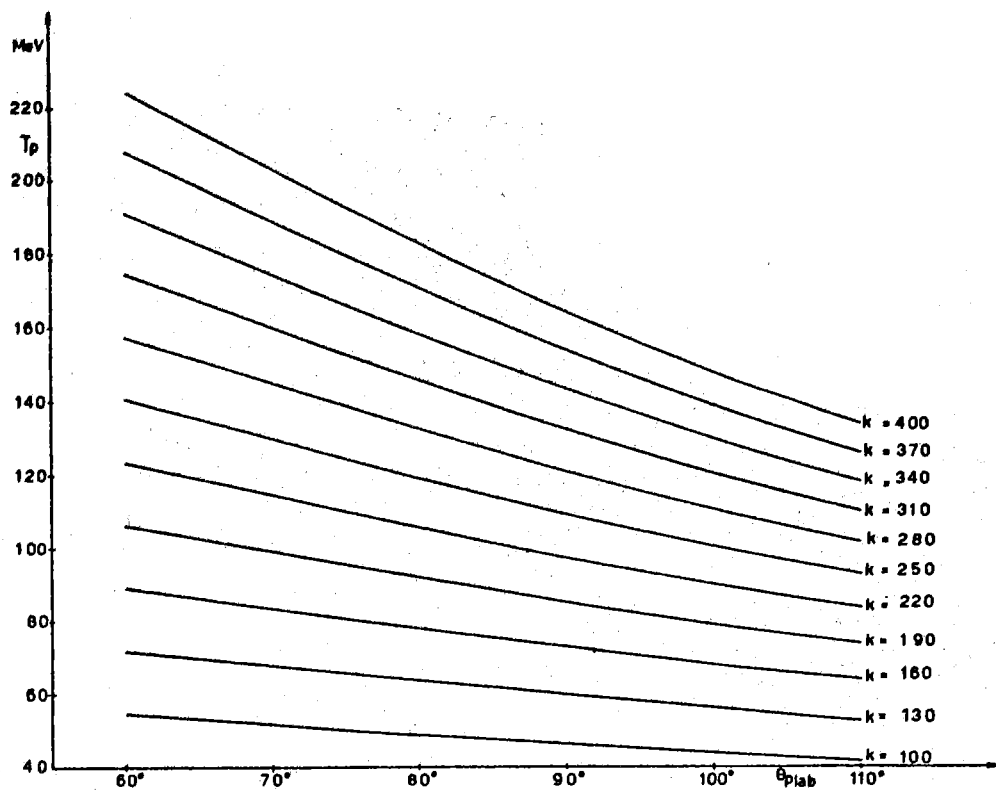


FIG. 4 - The kinematics for photodisintegration of the deuteron (f, d)

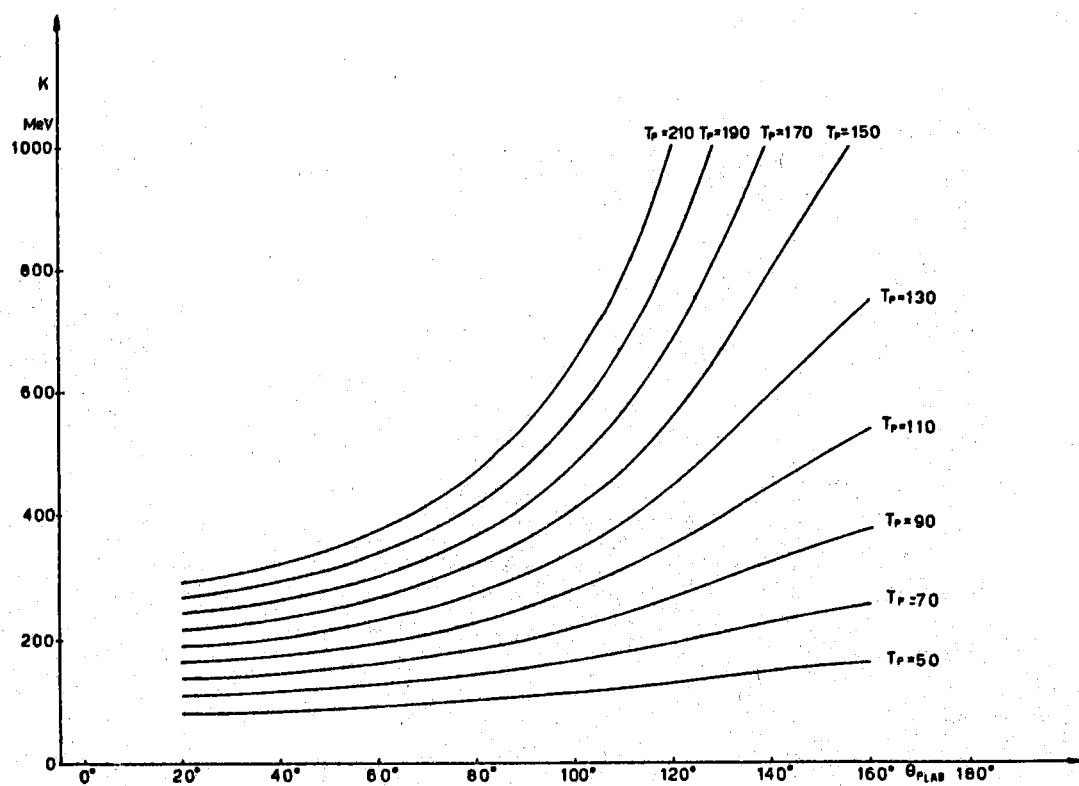


FIG. 5 - Laboratory photon energy for photodisintegration as a function of proton laboratory angle at various proton kinetic energy.

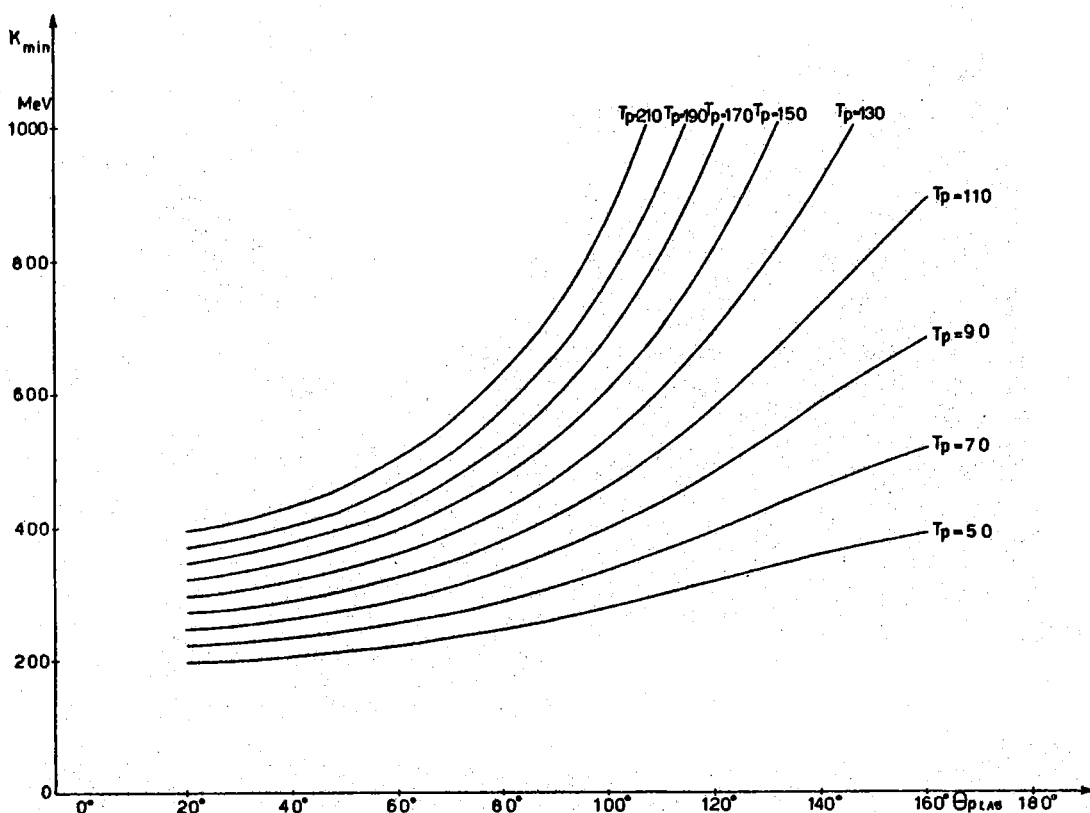


FIG. 6 - Minimum photon energy which produces a proton with kinetic energy  $T_p$  at angle  $\theta_{p,\pi}$  in the (f. p.  $\pi$ ).

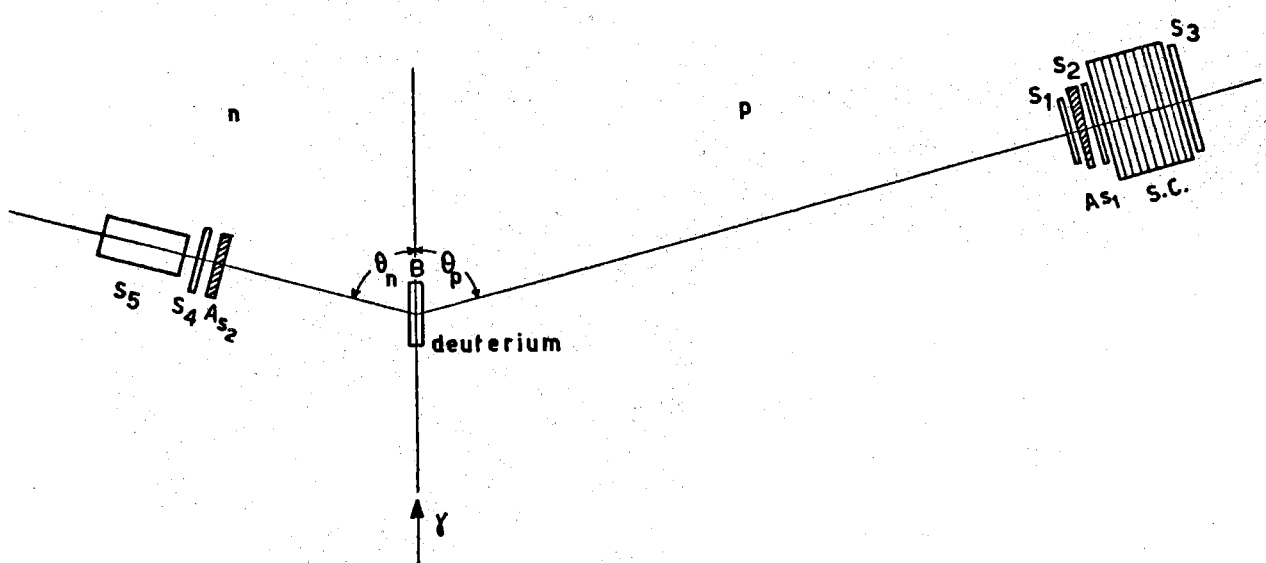


FIG. 7 - Experimental apparatus.

The expected proton energy resolution of the spark chamber is  $\pm 0.5$  MeV per gap for incoming protons in the energy range  $100 \pm 200$  MeV.

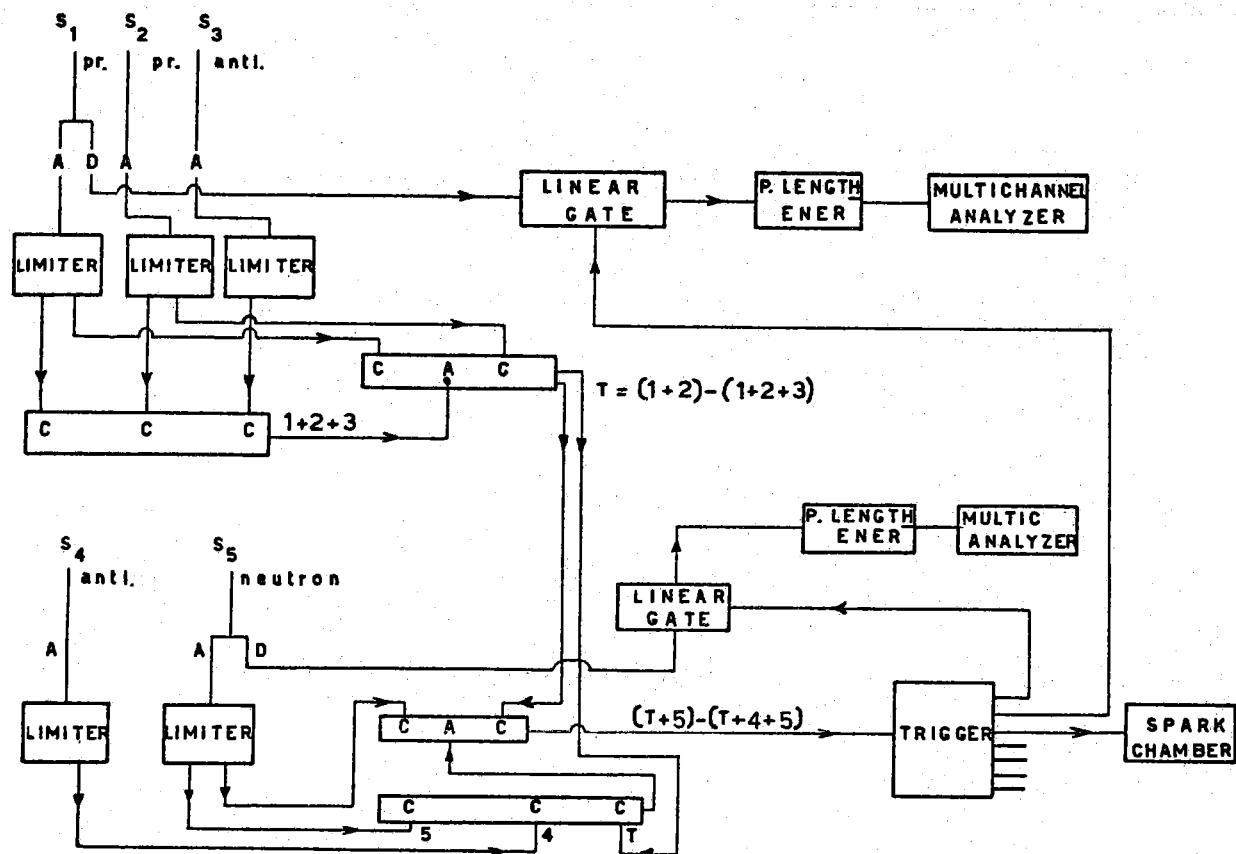


FIG. 8 - Electronics blok scheme

The solid angles and the neutron counter efficiency have not been accurately estimated since ratios of cross sections are not affected by them (the proton telescope is about 10 msterad wide and the neutron counter efficiency is  $10 \pm 15\%$ : this helps in estimating the counting rate).

Eventually, the target is a liquid deuterium cilinder 15 cm long, 3 cm base diameter.

Due to the near proportionality of the  $\gamma$  ray energy to the proton kinetic energy, the crystal bremsstrahlung peak can be reproduced in the spark chamber S.C. as a peak in a curve counts versus range.

This allows a good energy calibration by comparison of the proton spectrum shape to the one obtained by a pair spectrometer, thanks to the sharpness of the peak on the high energy side. As shown in fig. 9a), 9b) the photon energy resolution can be estimated by this method to be  $\pm 15$  MeV.

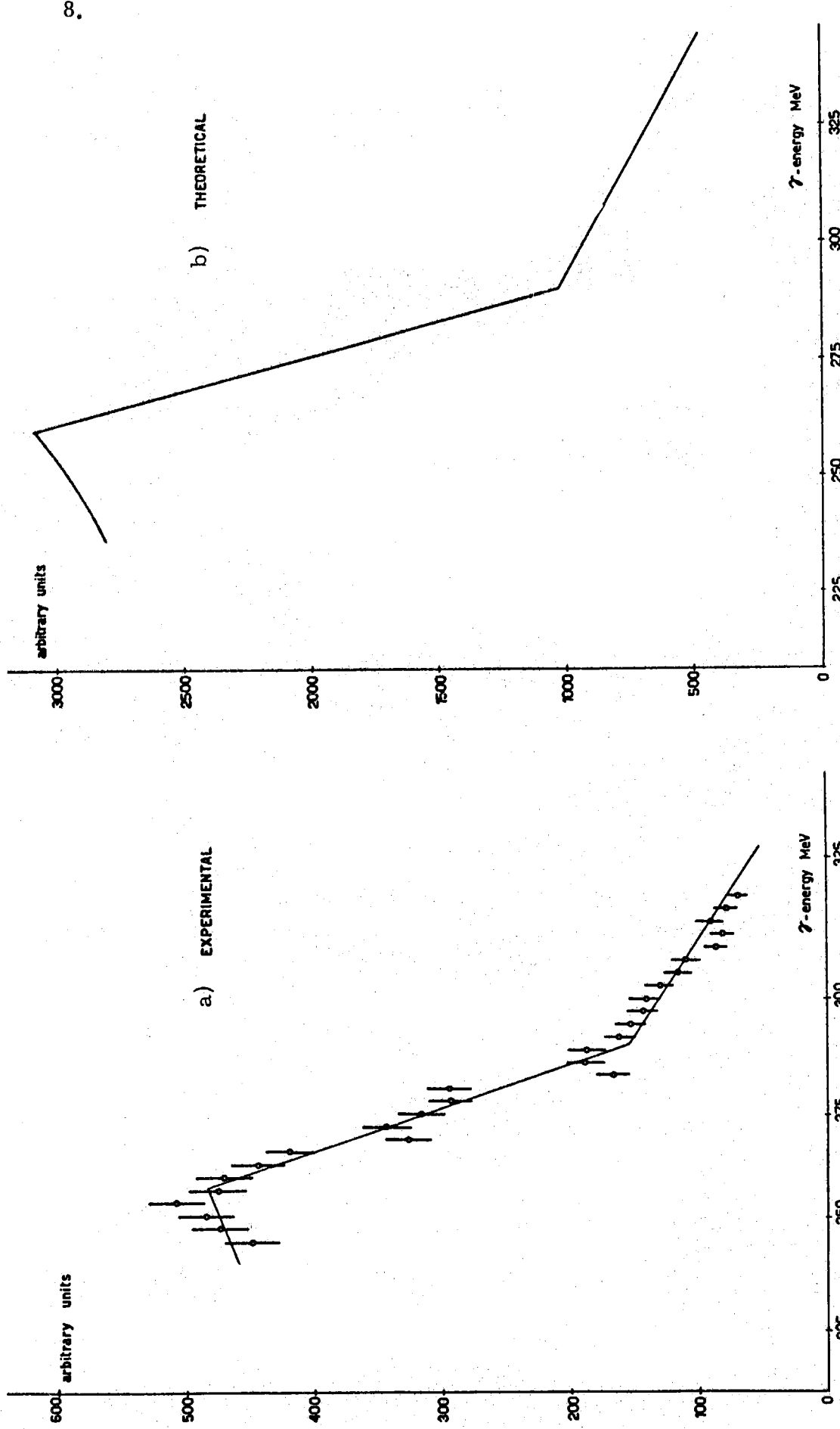


FIG. 9 - a) e b) Bremsstrahlung spectrum from the diamond around a coherent peak as seen by the proton range spectrum in the spark chamber. Resolution is given by comparison with the expected spectrum (b).

### 3 - RESULTS -

By using the experimental apparatus described above, 3 points have been measured giving the asymmetry function  $\Sigma(\theta, k)$  at  $\theta = 90^\circ$  (c.m. proton angle) and  $k = 260, 285, 308$  MeV (laboratory  $\gamma$  ray energy).

The polarization  $P$  of the  $\gamma$  rays has been computed according to Barbiellini et al. (8); error estimates on  $P$  have not been included.

The statistical error on  $\Sigma$  has been computed by

$$(2) \quad \frac{\delta \Sigma}{\Sigma} = \frac{\sqrt{1 - (P\Sigma)^2}}{P\Sigma \sqrt{n}}$$

where  $n$  is the total number of counts. The results are shown in fig. 10.

In the same fig. 10 a quantity, we call  $\Sigma_\pi(k, \theta)$  is also plotted as a

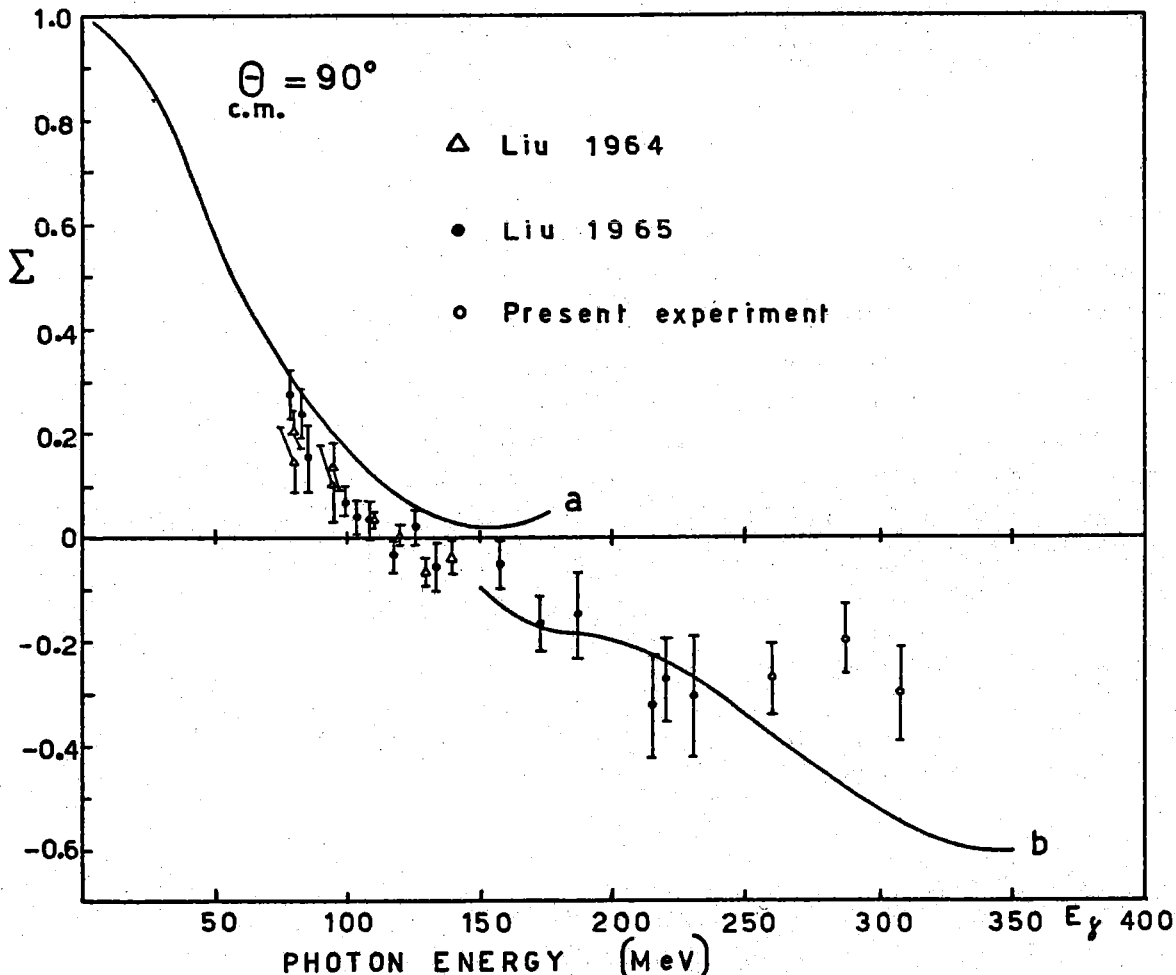


FIG. 10 - Experimental results for the asymmetry function  $\Sigma$  at  $90^\circ$  in the c.m. system. Symbols are as follows: hollow triangle, solid circle - Liu<sup>(7)</sup>; hollow circle-present experiment; Curve a is according to Breit et al<sup>(15)</sup>; Curve b is  $\Sigma_\pi$  as defined in eq. (3).

function of the  $\gamma$  ray energy, for  $\theta = 90^\circ$ .  $\sum_{\pi}$  is defined as follows

$$(3) \quad \sum_{\pi}(k, \theta) = \frac{1.8 \sum_{\pi^0}(k, \theta) + 2.4 \frac{d\sigma'_{\pi^+}(k, \theta)}{d\sigma'_{\pi^0}(k, \theta)} \sum_{\pi^+}(k, \theta)}{1.8 + 2.4 \frac{d\sigma'_{\pi^+}(k, \theta)}{d\sigma'_{\pi^0}(k, \theta)}}$$

where

$$(4) \quad \sum_{\pi^+(o)} = \frac{d\sigma'_{\pi^+(o)}(k, \theta) - d\sigma'_{\pi^+(o)}^L(k, \theta)}{d\sigma'_{\pi^+(o)}(k, \theta) + d\sigma'_{\pi^+(o)}^L(k, \theta)}$$

are the asymmetry functions of the  $\pi$  photoproduction process on protons from linearly polarized photon (11, 12, 13) and  $d\sigma'_{\pi^+(o)}(k, \theta)$  are the  $\pi$  photo production differential cross sections on protons from unpolarized photons.

$\theta$  is the C.M.S. angle between proton and incident  $\gamma$  momentum. The  $\gamma$  ray energy in the laboratory system  $k$  corresponds to the same photon energy in the  $\gamma$ -nucleon C.M.S. and  $\gamma$ -deuteron C.M.S.

The coefficients 1.8 and 2.4 in eq. (3), according to the Wilson model, take into account the contribution of all the  $\pi$  photoproduction processes on nucleon to the deuteron photodisintegration cross section.

Since the total photodisintegration cross section is well fitted by a suitable combination of photoproduction data, it seems likely that the asymmetry functions are related in a similar way. There is no precise theoretical basis in performing this interpolation: however, the curve shown in fig. 10 calculated according to the Wilson mixture shows a remarkable qualitative agreement.

#### ACKNOWLEDGEMENTS -

We want to thank Mr. Bruno Bartoli for his collaboration during the development of this work.

#### REFERENCES -

- (1) - M.E. Toms, U.S. Naval Res. Lab. Bibl. 24 (1965).
- (2) - F. Partovi, Ann. Phys. 27, 79 (1964).
- (3) - M. Le Bellac, F.M. Renard and J. Tran Thanh Van, Nuovo Cimento 33, 594 (1964).
- (4) - N. Austern, Phys. Rev. 100, 1522 (1955).

- (5) - F. Zachariasen, Phys. Rev. 101, 371 (1956).
- (6) - R.R. Wilson, Phys. Rev. 104, 218 (1956).
- (7) - F.F. Liu, Phys. Letters 11, 306 (1964), Phys. Rev. 138, B1443 (1965).
- (8) - G. Barbiellini, G. Bologna, G. Diambrini and G.P. Murtas, Phys. Rev. Letters 9, 396 (1962).
- (9) - R.E. Taylor and R.F. Mozley, Phys. Rev. 117, 835 (1960).
- (10) - D.M. White, R.M. Schechtman and B.M. Chasan, Phys. Rev. 120, 614 (1960).
- (11) - G. Barbiellini, G. Bologna, J. De Wire, G. Diambrini, G.P. Murtas and G. Sette, Proceedings of Dubna Conference 1964.
- (12) - A. Donnachie and G. Shaw, Preprint.
- (13) - P. Gorenstein, M. Grilli, M. Nigro, E. Schiavuta, F. Soso, P. Spillantini and V. Valente, Phys. Letters 19, 157 (1965).
- (14) - L. Schiff, Phys. Rev. 78, 733 (1950).
- (15) - M.I. Rustgi, W. Zernik, G. Breit and D.J. Andrews, Phys. Rev. 120, 1881 (1960).